

# **An Organic-Ligand-Free Crescent Thermo-chromic Luminescent Cuprous Iodide Trinuclear Cluster: Cluster Centered Emission and Configuration Distortion with Temperature**

Shi-Li Li, Fu-Qiang Zhang, Xian-Ming Zhang

**Materials and Methods.** The FT-IR spectra were recorded from KBr pellets in range 400-4000  $\text{cm}^{-1}$  on a Perkin-Elmer Spectrum BX FT-IR spectrometer. Elemental analysis was performed on a Vario EL-II elemental analyzer. XRPD data were recorded in a Bruker D8 ADVANCE X-ray powder diffractometer ( $\text{Cu}_{\text{K}\alpha}$ ,  $\lambda = 1.5418$  Å). UV-vis absorption was monitored with a U-3310 spectrophotometer. Crystalline SHG signals were measured based on the method from Kurtz and Perry. Since SHG efficiencies strongly depend on particle size, crystalline samples were ground and sieved into the following particle size ranges: 25-63, 63-80, 80-125, 125-150, 150-200, 200-300 $\mu\text{m}$ . The samples were pressed between glass microscope cover slides and secured with tape in a 1-mm thick aluminum holder with an 8-mm diameter hole. To compare with the relevant well-known SHG materials, crystalline KDP were also ground and sieved into the same particle size ranges. The samples were then placed in a light-tight box and irradiated with a pulsed laser. The measurements were done with a Q-switched Nd: YAG laser at 532 nm for UV SHG. A cutoff filter was used to limit background flash-lamp light on the sample, and an interference filter ( $530\pm 10\text{nm}$ ) was used to select the second harmonic for detection with a photomultiplier tube attached to an oscilloscope. This procedure was then repeated with the standard nonlinear

optical materials KDP, and the ratio of the second-harmonic intensity outputs was calculated.

Steady-state photoluminescence spectra and lifetime measurements were measured by a single-photon counting spectrometer using an Edinburgh FLS920 spectrometer equipped with a continuous Xe900 xenon lamp, a mF900 microsecond flash lamp, a red-sensitive Peltier-cooled Hamamatsu R928P photomultiplier tube (PMT), and a closed Janis CCS-350 Optical Refrigerator System. The corrections of excitation and emission for the detector response were performed ranging from 200 to 900 nm. Temperature-dependent measurements were carried out in a JANIS SHI-4S-1 cold head cooled with HC-4A compression engine. The data were analyzed by iterative convolution of the luminescence decay profile with the instrument response function using the software package provided by Edinburgh Instruments. Lifetime data were fitted with triple-exponential-decay functions. The quantum yields were measured by use of an integrating sphere with Edinburgh Instrument FLS920 spectrometer.

### **Synthesis.**

Synthesis of  $[\text{Bu}_2\text{DABCO}]_3[\text{Cu}_3\text{I}_6]_2$  (**1**): A mixture of  $\text{CuCl}_2 \cdot 2\text{H}_2\text{O}$  (1 mmol, 0.170 g), KI (2 mmol, 0.334 g),  $\text{DABCO} \cdot 6\text{H}_2\text{O}$  (0.5 mmol, 0.113 g) and BuOH (10 mL) was stirred and adjusted by  $\text{CH}_3\text{COOH}$  to pH ca. 3, and then sealed in a 25-ml Teflon-lined stainless container and heated to  $130^\circ\text{C}$  for 10 days. With a cooling rate of  $5^\circ\text{C min}^{-1}$  to room temperature, generated yellowish column crystals of **1** in 62% yield were recovered. Anal. Calc. for  $\text{C}_{21}\text{H}_{45}\text{Cu}_3\text{I}_6\text{N}_3$  **1**: C, 19.53; H, 3.51; N, 3.25.

Found: C, 17.32; H, 3.62; N, 3.35. IR(KBr,  $\text{cm}^{-1}$ ): 3451s, 2939w, 2861w, 2371w, 1631m, 1381m, 1259w, 1111s, 840w, 799w, 620s, 539w.

**Crystallographic studies.** X-ray single-crystal diffraction data for **1** were collected on a Agilent Technologies Gemini EOS diffractometer at ten temperatures (100K, 150K, 200K, 250K, 298 K, 373K, 393K, 403K, 423K and 473K) using Mo K $\alpha$  radiation ( $\lambda = 0.71073 \text{ \AA}$ ). The program SAINT was used for integration of diffraction profiles, and the program SADABS was used for absorption correction. The structures were solved with XS structure solution program by direct method and refined by full-matrix least-squares technique using Olex2. All non-hydrogen atoms were refined with anisotropic thermal parameters. Hydrogen atoms of organic cations were generated theoretically onto the specific carbon atoms, and refined isotropically with fixed thermal factors below 373K. However, due to large thermal vibration for atoms at high temperature, non-hydrogen atoms could not be refined very well above 393K. Hydrogen atoms were not accurately generated onto the specific carbon atoms of organic cations. Thus, the cif data for **1** above 393K are only used as references but not as new data delivered to the Cambridge Structural Database (CSD).

### **Calculation Details**

All the calculations have been performed with the ADF program package. The BP86 exchange-correlation functional was used throughout. A TZ2P basis set was used for all the atoms, along with the zero-order regular approximation (ZORA) to account for the relativistic effect. The same basis set was used for both geometry optimizations and TDDFT calculations. To check the effect of basis set expansion and

quality on the calculated geometrical structures, geometry optimizations and frequency calculations of the singlet ground state and the lowest triplet excited state were performed, and no imaginary frequency exists. In ADF, a scalar relativistic TDDFT calculation included spin-orbit coupling (SOC-TDDFT) can tackle the singlet-triplet excitations of closed-shell system. To check the effect of solvation on the calculated optical absorption spectra, we performed TDDFT calculations (singlet  $\rightarrow$  triplet) with the triplet optimized geometry, including solvation effects by means of the none equilibrium implementation of the polarizable continuum model; as in the experimental conditions, the chosen solvent was dicloromethane.

**Table S1.** Crystallographic Data and Structure Refinement for **1** at variable temperatures

<b>T/K</b>	<b>100</b>	<b>150</b>	<b>200</b>
Space group	P22 <sub>1</sub> 2 <sub>1</sub>	P22 <sub>1</sub> 2 <sub>1</sub>	P22 <sub>1</sub> 2 <sub>1</sub>
a (Å)	8.52016(18)	8.5342(4)	8.5719(8)
b (Å)	31.2866(8)	31.3102(12)	31.305(3)
c (Å)	13.2813(3)	13.3245(5)	13.4018(7)
$\alpha$ (deg)	90	90	90
$\beta$ (deg)	90	90	90
$\gamma$ (deg)	90	90	90
V (Å <sup>3</sup> )	3540.36(14)	3560.4(2)	3596.3(5)
Z	4	4	4
$\rho_{\text{calc.}}$ (g cm <sup>-3</sup> )	2.423	2.337	2.387
$\mu$ , (mm <sup>-1</sup> )	7.033	6.989	6.930
$F(000)$	2388	2304	2389
Reflections	24663/6233	9619/5767	4824/3932
$T_{\text{max}}/T_{\text{min}}$	0.7200/0.1562	0.7213/0.1573	0.7232/0.1589
Data/parameters	6233/0/335	5767/0/335	3932/0/333

S	1.108	1.108	1.030
$R_1^a$	0.0299	0.0332	0.0295
$wR_2^p$	0.0611	0.0706	0.0573
$\Delta\rho_{\max}/\Delta\rho_{\min}(eA^{-3})$	1.579/-2.380	1.374/-1.913	0.602/-0.708

---

<b>250</b>	<b>298</b>	<b>373</b>	<b>393</b>
P22 <sub>1</sub> 2 <sub>1</sub>			
8.6000(5)	8.6034(3)	8.6312(5)	8.6559(6)
31.212(2)	31.2560(14)	31.2048(19)	31.2083(19)
13.5723(8)	13.5945(6)	13.6767(8)	13.7178(8)
90	90	90	90
90	90	90	90
90	90	90	90
3643.2(4)	3655.7(3)	3683.6(4)	3705.7(4)
4	4	4	4
2.355	2.346	2.330	2.334
6.834	6.808	6.766	6.716
2388	2387	2389	2208
10968/6101	13534/7301	11568/6273	11924/6288
0.7717/0.1379	0.7724/0.1386	0.7284/0.1329	0.7300/0.1341
6101/0/341	7301/1/342	6273/15/336	6288/5/332
1.073	1.033	1.1041	1.050
0.0450	0.0517	0.0633	0.0557
0.0934	0.1163	0.1444	0.1573
0.629/-0.922	1.008/-0.831	0.745/-0.701	1.003/-0.640

---

<b>403</b>	<b>423</b>	<b>473</b>
Pmnn	Pnnm	Pnnm
8.6716(9)	8.6732(6)	8.6968(10)
31.202(2)	31.2247(2)	31.325(4)
13.7436(8)	13.7796(10)	13.8487(14)
90	90	90
90	90	90

90	90	90
3718.6(5)	3734.4(4)	3772.8(8)
4	4	4
2.183	2.217	2.194
6.690	6.665	6.597
2161	2208	2208
15608/5610	13899/5492	11275/4614
0.7309/0.1348	0.7764/0.1422	0.7339/0.1439
5610/1/217	5492/0/217	4614/0/214
1.038	1.028	1.016
0.0743	0.0653	0.0754
0.2487	0.1948	0.1883
0.614/-0.916	0.640/-0.853	0.581/-0.889

$${}^a R_1 = \frac{\sum ||F_o| - |F_c||}{\sum |F_o|} \cdot {}^b wR_2 = \left[ \frac{\sum [w(F_o^2 - F_c^2)^2]}{\sum [w(F_o^2)]} \right]^{1/2}$$

**Table S2.** Cu...Cu distances[Å] of **1** at variable temperatures.

Cu...Cu	<b>100K</b>	<b>150K</b>	<b>200K</b>	
Cu(1) ...Cu(2)	2.53995(17)	2.5310(6)	2.5548(7)	
Cu(1) ...Cu(3)	2.55053(16)	2.5462(6)	2.5278(9)	
Cu(1')...Cu(2)	2.4376(6)	2.4589(15)	2.4983(11)	
Cu(1')...Cu(3)	2.4806(7)	2.4831(16)	2.4579(15)	
mean	2.50217	2.5048	2.5097	
	<b>250K</b>	<b>298K</b>	<b>373K</b>	<b>393K</b>
	2.5081(4)	2.555(7)	2.5968(2)	2.537(9)
	2.5475(4)	2.511(8)	2.5433(2)	2.491(12)
	2.4779(4)	2.513(7)	2.4901(2)	2.512(17)
	2.5162(4)	2.477(8)	2.43841(18)	2.454(16)
	2.5124	2.5140	2.5172	2.502

Cu...Cu	<b>403K</b>	<b>423K</b>	<b>473K</b>
Cu(1) ...Cu(2)	2.512(4)	2.449(4)	2.448(5)
Cu(1) ...Cu(3)	2.453(5)	2.519(4)	2.525(5)
mean	2.483	2.484	2.487

**Table S3.** Cu-I distances[Å] of **1** at various temperatures.

	<b>100K</b>	<b>150K</b>	<b>200K</b>
Cu(1)-I(1)	2.50319(15)	2.4993(5)	2.5137(7)
Cu(1)-I(2)	2.50939(14)	2.5069(5)	2.5032(9)
Cu(1)-I(3)	2.67247(14)	2.6966(6)	2.7040(7)
Cu(1')-I(2)	2.4905(6)	2.5194(15)	2.5224(15)
Cu(1')-I(1)	2.5302(6)	2.5259(15)	2.5138(12)
Cu(1')-I(4)	2.8487(7)	2.7965(16)	2.8086(12)
Cu(2)-I(5)	2.55818(12)	2.5526(4)	2.5322(4)
Cu(2)-I(4)	2.65364(12)	2.6744(4)	2.7129(6)
Cu(2)-I(2)	2.78053(13)	2.7881(4)	2.7167(5)
Cu(2)-I(3)	2.81627(12)	2.8037(4)	2.7955(5)
Cu(3)-I(6)	2.53943(12)	2.5323(4)	2.5490(6)
Cu(3)-I(4)	2.67833(13)	2.6986(5)	2.6989(5)
Cu(3)-I(1)	2.70765(13)	2.7094(4)	2.7973(4)
Cu(3)-I(3)	2.81390(13)	2.8015(5)	2.7967(5)

Symmetry codes: a) x,-y+1,-z+1

	<b>250K</b>	<b>298K</b>	<b>373K</b>	<b>393k</b>
	2.4903(3)	2.512(7)	2.5130(2)	2.496(9)
	2.5119(3)	2.495(6)	2.4871(2)	2.461(7)
	2.7592(4)	2.761(13)	2.7672(2)	2.89(3)
	2.5340(4)	2.519(7)	2.51602(19)	2.568 (17)

2.5189(4)	2.538(9)	2.53346(17)	2.58(2)
2.7478(4)	2.756(19)	2.77351(19)	2.62(4)
2.5299(3)	2.5228(18)	2.51479(14)	2.511(2)
2.7488(2)	2.741(2)	2.75420(14)	2.768(3)
2.8022(3)	2.7248(19)	2.71921(16)	2.717(2)
2.7844(2)	2.776(2)	2.78078(15)	2.772(3)
2.5172(2)	2.537(2)	2.52745(17)	2.522(2)
2.7388(2)	2.751(2)	2.77210(15)	2.779 (3)
2.7263(2)	2.802(2)	2.81175(19)	2.820(3)
2.7745(2)	2.789(2)	2.78091(15)	2.778(3)

Symmetry codes: a) x,-y+1,-z+1

	<b>403K</b>	<b>423K</b>	<b>473K</b>
Cu(1)-I(1)	2.484(3)	2.467(3)	2.466(4)
Cu(1)-I(2)	2.462(3)	2.486(3)	2.491(4)
Cu(1)-I(3)	3.046(3)	3.044(2)	3.049(3)
Cu(1)-I(3a)	3.046(3)	3.044(2)	3.049(3)
Cu(2)-I(2)	2.716(3)	2.831(3)	2.853(4)
Cu(2)-I(3)	2.771(2)	2.777(2)	2.780(3)
Cu(2)-I(3a)	2.771(2)	2.777(2)	2.780(3)
Cu(2)-I(4)	2.512(3)	2.520(3)	2.515(4)
Cu(3)-I(1)	2.820(4)	2.721(3)	2.734(4)
Cu(3)-I(3)	2.781(2)	2.7738(18)	2.778(3)
Cu(3)-I(3a)	2.781(2)	2.7738(18)	2.778(3)
Cu(3)-I(5)	2.519(3)	2.510(2)	2.509(3)

Symmetry codes: a) -x+1,y,z b) -x,y,z c) -x,-y+1,-z+1 d) x,-y+1,-z+1

**Table S4.** All Spin-Orbital Coupling Excitation Energies

Excitation	E/eV	oscillator strengths (a.u.)
singlet → triplet	0.89013	0.2917E-07

singlet → singlet    1.04211    0.3135E-03

---

**Table S5.** Experimental and calculated Cu...Cu and Cu-I distances[Å] of **1**.

<b>Experimental at 298K</b>		<b>Ground State</b>		<b>Excited State</b>	
Cu(1)-Cu(2)	2.555(7)	Cu(1)-Cu(2)	2.4997	Cu(1)-Cu(2)	2.4574
Cu(1)-Cu(3)	2.511(8)	Cu(1)-Cu(3)	2.4997	Cu(1)-Cu(3)	2.4554
Cu(1)-I(2)	2.495(6)	Cu(1)-I(2)	2.5685	Cu(1)-I(2)	2.5830
Cu(1)-I(1)	2.512(7)	Cu(1)-I(1)	2.5685	Cu(1)-I(1)	2.5823
Cu(1)-I(3)	2.761(13)	Cu(1)-I(3)	2.6664	Cu(1)-I(3)	4.0452
Cu(2)-I(5)	2.5228(18)	Cu(2)-I(5)	2.5763	Cu(2)-I(5)	2.5493
Cu(2)-I(2)	2.7248(19)	Cu(2)-I(2)	2.8219	Cu(2)-I(2)	3.9751
Cu(2)-I(4)	2.741(2)	Cu(2)-I(4)	2.6394	Cu(2)-I(4)	2.8457
Cu(2)-I(3)	2.776(2)	Cu(2)-I(3)	2.8722	Cu(2)-I(3)	2.7015
Cu(3)-I(6)	2.537(2)	Cu(3)-I(6)	2.5763	Cu(3)-I(6)	2.5489
Cu(3)-I(4)	2.751(2)	Cu(3)-I(4)	2.6394	Cu(3)-I(4)	2.7054
Cu(3)-I(3)	2.789(2)	Cu(3)-I(3)	2.8722	Cu(3)-I(3)	2.8547
Cu(3)-I(1)	2.802(2)	Cu(3)-I(1)	2.8219	Cu(3)-I(1)	3.9126

**Table S6.** Coordinates of optimized singlet Cu<sub>3</sub>I<sub>6</sub><sup>3-</sup>

Cu(1)	-1.237266	0.543936	0.000000
Cu(2)	0.379508	-0.229336	-1.742645
Cu(3)	0.379508	-0.229336	1.742645
I(1)	-2.343883	0.256356	2.299977
I(2)	-2.343883	0.256356	-2.299977
I(3)	1.020889	1.961870	0.000000
I(4)	0.662182	-2.191389	0.000000
I(5)	1.751266	-0.215620	-3.923322
I(6)	1.751266	-0.215620	3.923322

**Table S7.** Coordinates of optimized triplet  $\text{Cu}_3\text{I}_6^{3-}$

Cu(1)	0.020724	1.390643	0.017007
Cu(2)	1.155185	-0.785322	0.147113
Cu(3)	-1.170477	-0.740833	-0.241822
I(1)	-1.719232	2.822242	1.278527
I(2)	1.774674	2.950715	-1.060919
I(3)	-0.207336	-2.075093	2.090808
I(4)	0.158308	-2.067384	-2.189654
I(5)	3.669889	-0.829196	0.563189
I(6)	-3.685963	-0.738132	-0.653120

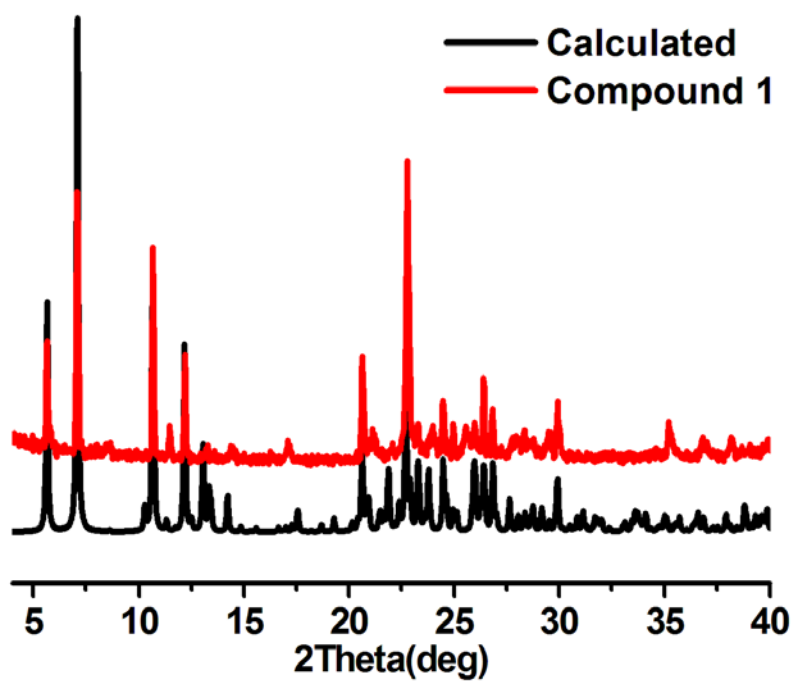


**Figure S1.** PXRD of compound **1** at room temperature and calculated from the single crystal data recorded at room temperature.

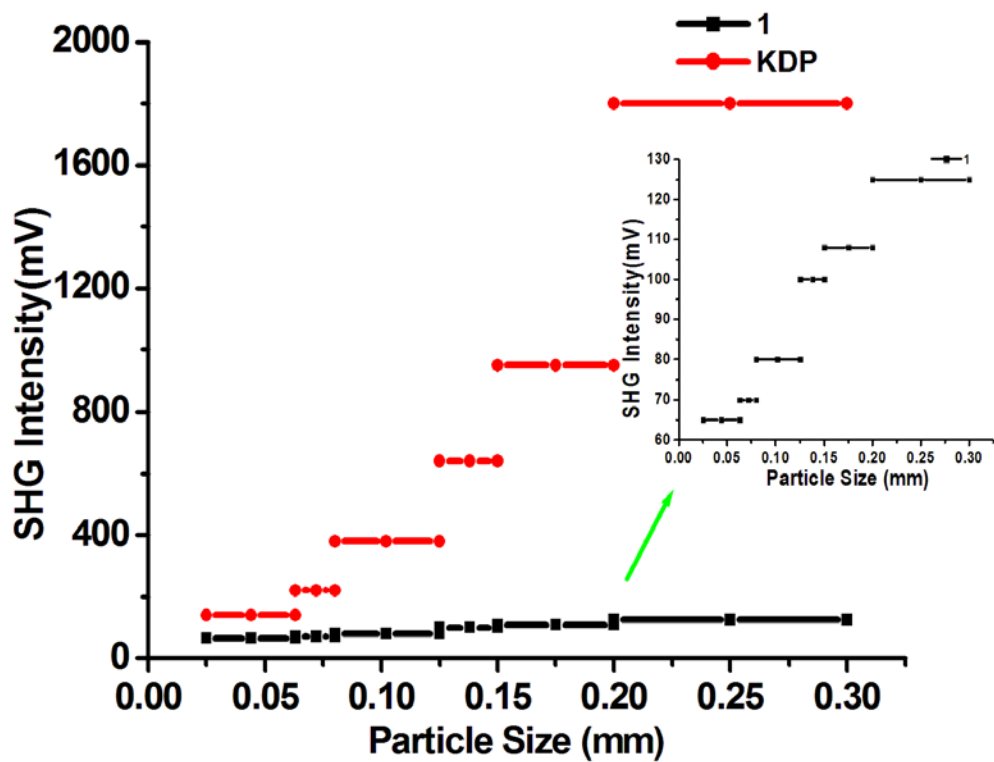


Figure S2. SHG signals of 1 and KDP.

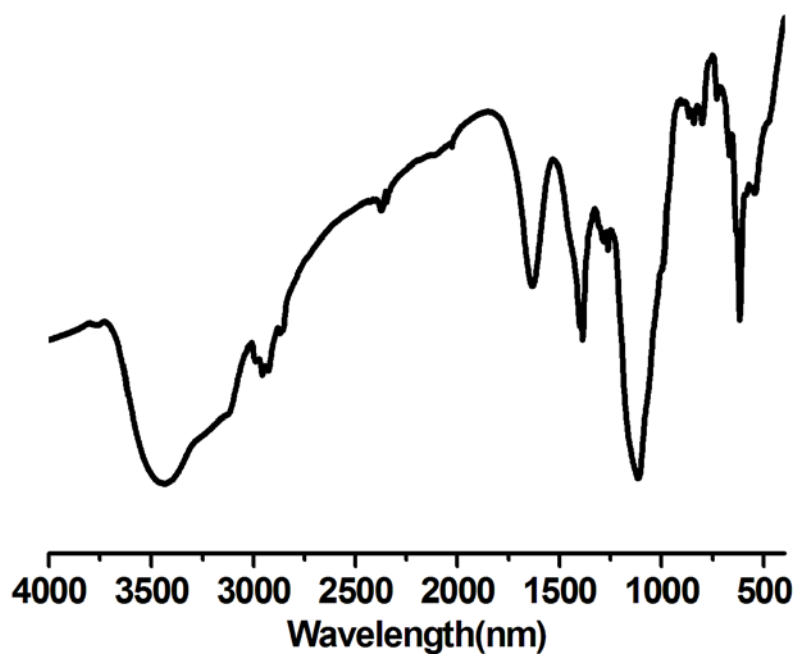


Figure S3. IR Spectra of compound 1.

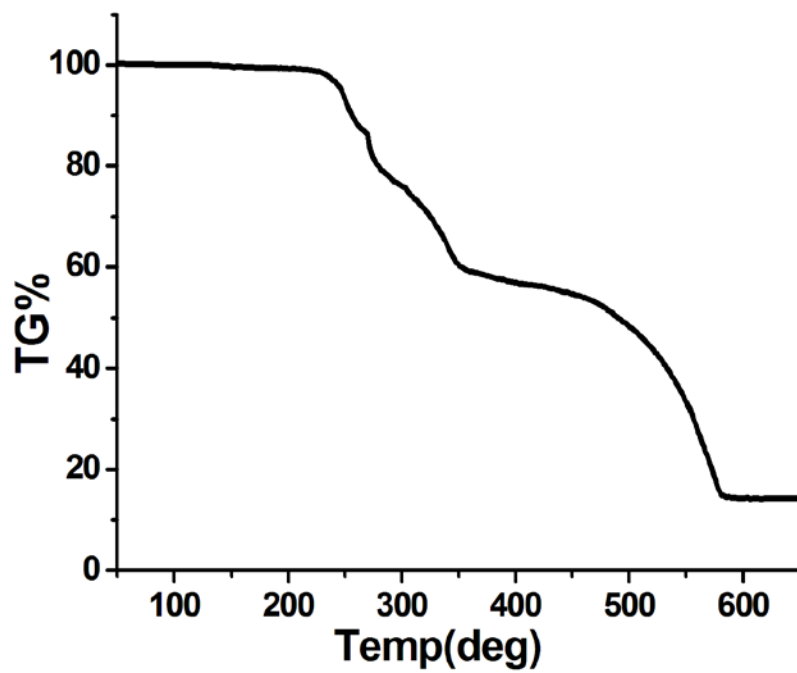


Figure S4. TGA curves of **1** in air atmosphere.

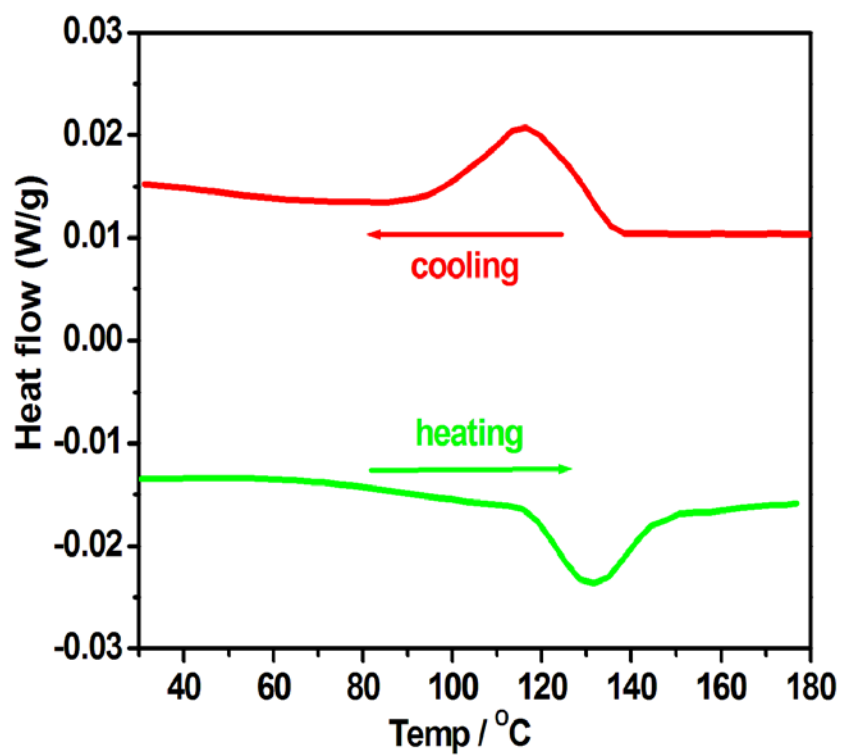
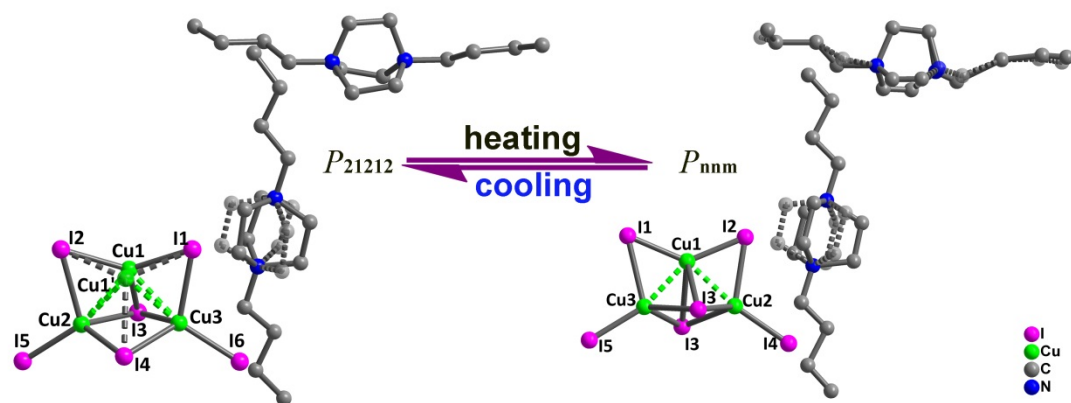
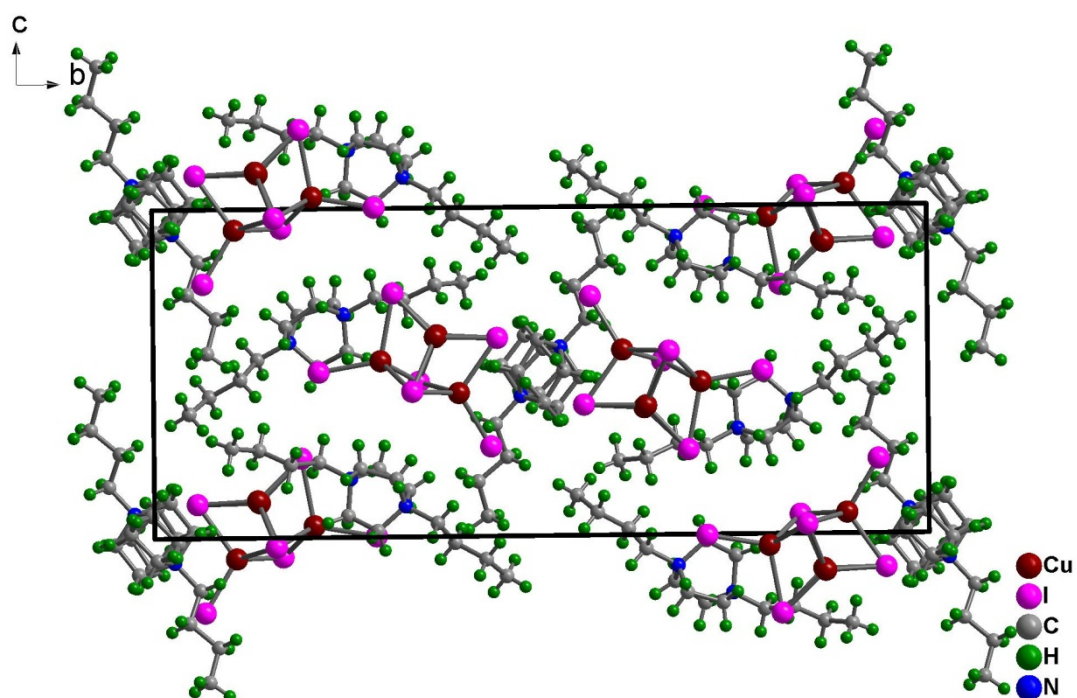


Figure S5. DSC curves of **1**.



**Figure S6.** View of the molecular structure of **1** before and after phase transition.



**Figure S7.** Packing arrays of *N,N'*-dibutyl-1,4-diazabicyclo-[2.2.2]octane and  $\text{Cu}_3\text{I}_6^{3-}$  clusters in low temperature phase **1** viewed along the *a*-axis direction.

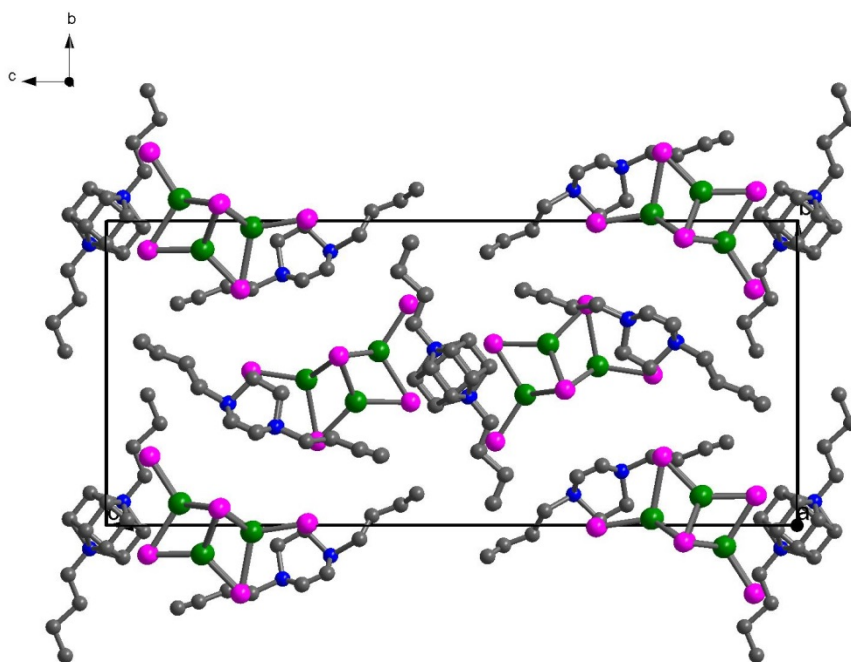


**Figure S8.** Packing arrays of *N,N'*-dibutyl-1,4-diazabicyclo-[2.2.2]octane and  $\text{Cu}_3\text{I}_6^{3-}$  clusters in high temperature phase **1** viewed along the *a*-axis direction.

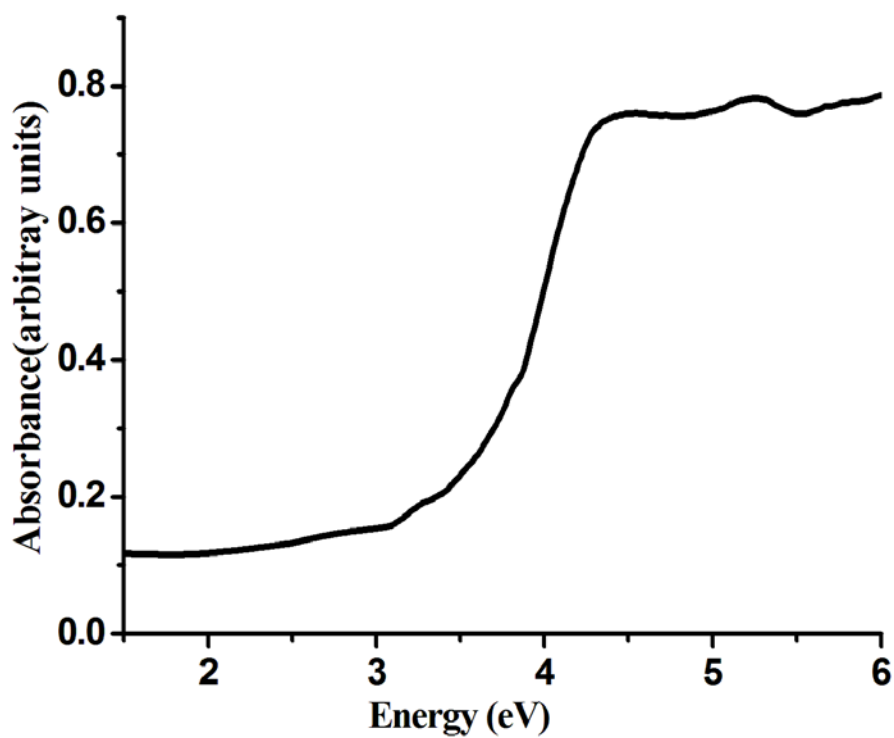


**Figure S9.** UV-vis diffuse reflectance spectrum of **1**.

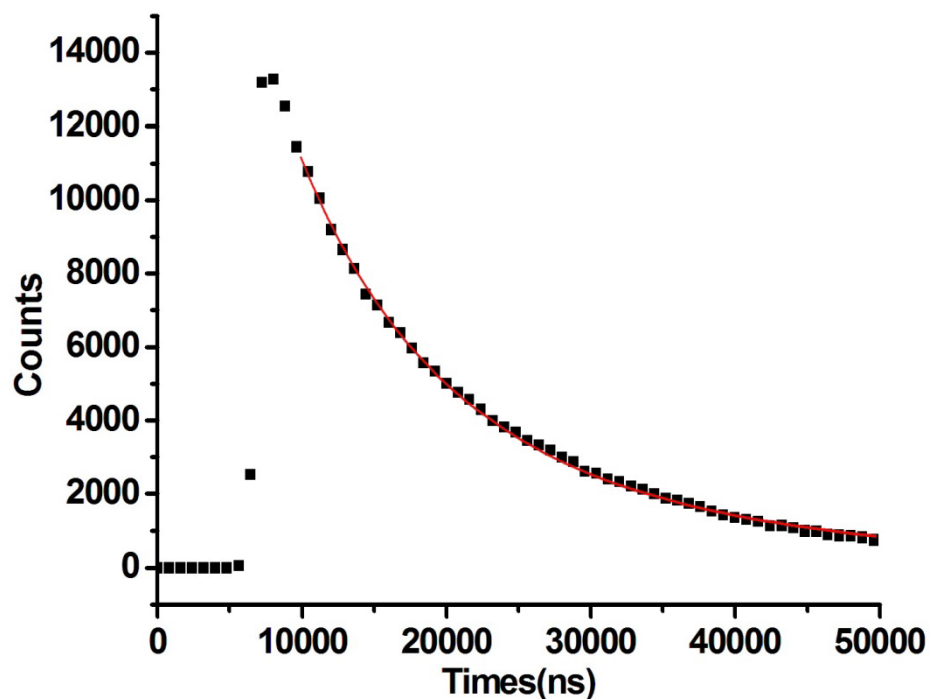


**Figure S10** Emission lifetime curves and corresponding fits for **1** at room temperature.

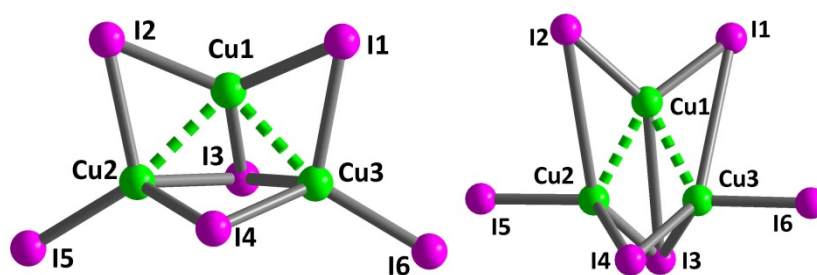


**Figure S11** the calculated ground state and excited state configurations of trinuclear  $\text{Cu}_3\text{I}_6^{3-}$  cluster.

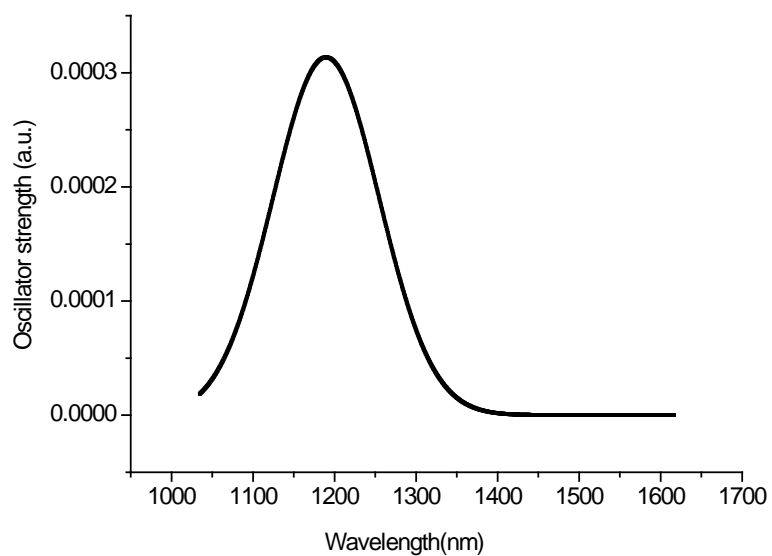


**Figure S12.** Oscillator strength of calculated of singlet  $\rightarrow$  triplet excitation of  $\text{Cu}_3\text{I}_6^{3-}$

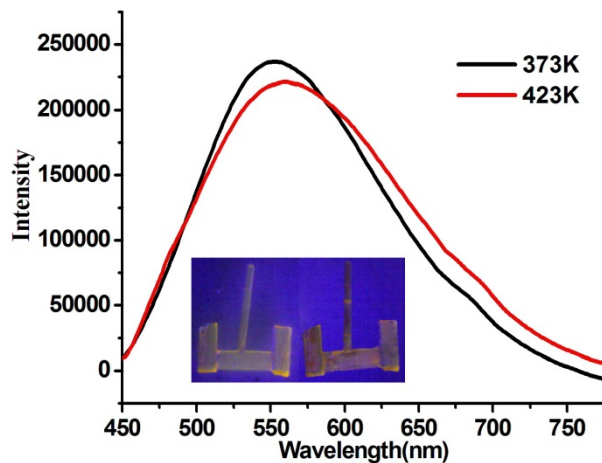


**Figure S13.** The luminescence spectra at 373K and 423K in the solid state. (Insert: Photos of the crystal samples at 373K (left) and at 423K (right) under 365nm UV lamp irradiation)

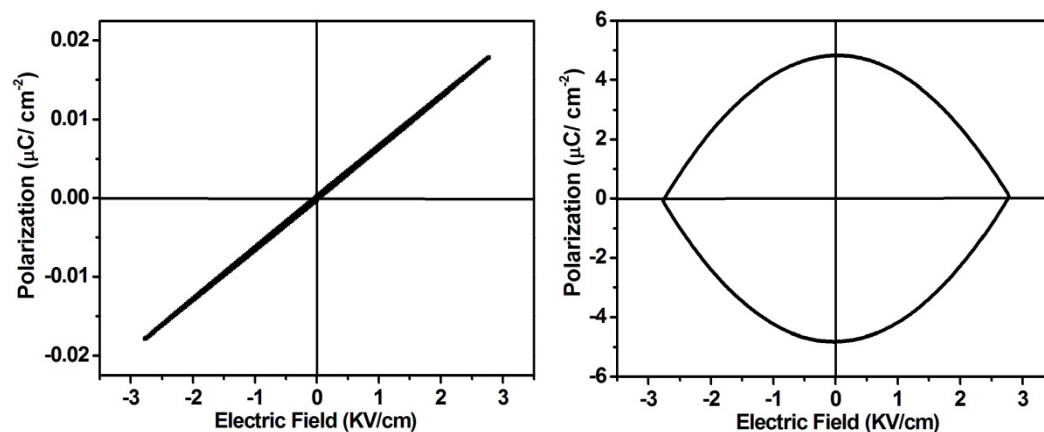


**Figure S14.** Polarization curve of a pellet of powder of compound **1** at room temperature (left) and at 423K (right).